atmosphere

MDPI

Article

Influence of Meteorological Conditions and Aerosol Properties on the COVID-19 Contamination of the Population in Coastal and Continental Areas in France: Study of Offshore and Onshore Winds

Jacques Piazzola [1,*], William Bruch [1], Christelle Desnues [1], Philippe Parent [2], Christophe Yohia [3] and Elisa Canepa [4]

[1] Mediterranean Institute of Oceanography (MIO UM 110), University of Toulon, CEDEX 09, 83041 Toulon, France; william.bruch@mio.osupytheas.fr (W.B.); Christelle.DESNUES@univ-amu.fr (C.D.)
[2] CNRS, Aix-Marseille University, UMR 7325, box 913, CEDEX 09, 13288 Marseille, France; philippe.parent@univ-amu.fr
[3] OSU Institut Pytheas-SIP (UMS 3470), CNRS/INSU, University of Aix-Marseille (AMU), CEDEX 07, 13284 Marseille, France; christophe.yohia@univ-amu.fr
[4] Institute for the Study of Anthropical Impact and Sustainability in the Marine Environment, National Research Council, 16149 Genova, Italy; elisa.canepa@ias.cnr.it
* Correspondence: piazzola@univ-tln.fr; Tel.: +33-494142082

Abstract: Human behaviors probably represent the most important causes of the SARS-Cov-2 virus propagation. However, the role of virus transport by aerosols—and therefore the influence of atmospheric conditions (temperature, humidity, type and concentration of aerosols)—on the spread of the epidemic remains an open and still debated question. This work aims to study whether or not the meteorological conditions related to the different aerosol properties in continental and coastal urbanized areas might influence the atmospheric transport of the SARS-Cov-2 virus. Our analysis focuses on the lockdown period to reduce the differences in the social behavior and highlight those of the weather conditions. As an example, we investigated the contamination cases during March 2020 in two specific French areas located in both continental and coastal areas with regard to the meteorological conditions and the corresponding aerosol properties, the optical depth (AOD) and the Angstrom exponent provided by the AERONET network. The results show that the analysis of aerosol ground-based data can be of interest to assess a virus survey. We found that moderate to strong onshore winds occurring in coastal regions and inducing humid environment and large sea-spray production episodes coincides with smaller COVID-19 contamination rates. We assume that the coagulation of SARS-Cov-2 viral particles with hygroscopic salty sea-spray aerosols might tend to inhibit its viral infectivity via possible reaction with NaCl, especially in high relative humidity environments typical of maritime sites.

Keywords: aerosols; sea-spray; COVID-19; AERONET

Citation: Piazzola, J.; Bruch, W.; Desnues, C.; Parent, P.; Yohia, C.; Canepa, E. Influence of Meteorological Conditions and Aerosol Properties on the COVID-19 Contamination of the Population in Coastal and Continental Areas in France: Study of Offshore and Onshore Winds. *Atmosphere* **2021**, *12*, 523. https://doi.org/10.3390/atmos12040523

Academic Editors: Ole Hertel and Tareq Hussein

Received: 22 February 2021
Accepted: 13 April 2021
Published: 20 April 2021

1. Introduction

The COVID-19 escalation, which started at the beginning of 2020 due to the SARS-CoV-2 coronavirus, is causing serious consequences in our society in terms of health with hundred thousands of deaths but also in terms of economy because of the confinement decision that nearly stopped the industrial and commercial activities of a large number of countries. Since 2003, when the SARS-CoV was identified, very few studies and routine monitoring dealt with the role of coronaviruses in humans [1]. In anticipation of another crisis in the future, we need to improve our knowledge of the spread of the SARS-Cov-2 and of potentially similar viruses, to help our governments to develop strategies avoiding as much possible stopping human activities. Human behaviors probably represent the most

important causes of the virus propagation [2,3] nevertheless, the influence of atmospheric environmental parameters need to be investigated as well in view of this containing strategy development [4,5].

SARS-Cov-2 is thought to spread through natural respiratory activities—such as breathing, talking, coughing, and sneezing [6,7]. Even if the recent study of Balachandar et al. [8] described the fluid dynamics of exhalations and subsequent dispersion processes, in practice little is still known about the spread of the virus in the air and survival [9]. It has been demonstrated that the probability of airborne transmission due to respiratory aerosol is very low in outdoor conditions excluding public crowded areas [10] but this transmission mechanism is more relevant for indoor environments [11]. Indoor air is a mixture of indoor airborne pollutants from specific sources and outdoor air that penetrates indoors [12–14]. Therefore, the influence of the outdoor environmental parameters—like solar radiation, [15] temperature, humidity, wind characteristics, pollution and aerosols load, etc.—needs to be investigated as well [4,9].

We need to explain why relatively close areas with similar human behaviors and socioeconomic properties experience very different situations in terms of the virus propagation. In this case, the role of the environmental parameters needs to be studied. Among them, the atmospheric aerosol could have a strong, indirect impact through its role in respiratory diseases [16–18]. As an example, Conticini et al. [19] investigated the correlation between the high COVID-19 lethality and the atmospheric pollution in Northern Italy, in which PM10 and PM2.5 were included, and they concluded that the high level of pollution in that area should be considered an additional cofactor of the high lethality recorded. In addition, the atmospheric aerosols could have a strong, direct impact through interaction with virus aerosolization, which is an important air dispersal mechanism of infectious viruses [20]. The accurate estimation of the impact of the atmospheric aerosol properties on virus virulence and propagation, including SARS-CoV-2, is then an important scientific challenge [21–23].

Regular aerosol observations based on well-calibrated instruments have led to a better understanding of the aerosol properties. In recent years, these instruments have played an important role in the determination of the increase in anthropogenic aerosols and of the quantification of the natural aerosols emissions by means of long-term studies. Among them, the AErosol RObotic NETwork (AERONET) program (http://aeronet.gsfc.nasa.gov/, accessed on 19 February 2021) aims to provide a global distribution of aerosol optical properties and to validate satellite retrievals. This network of ground observations provides suitable data for trend analysis of the aerosol optical depth (AOD) at main wavelengths (440, 675, 870, and 1020 nm) based on continuous long-term observations with high temporal resolution as well as high accuracy [24,25].

To understand the influence of the aerosol composition and why the polluted areas are suspected to be more exposed to higher rates of contamination, [19] coastal regions are of particular interest to investigate since they are alternatively under influence of continental and marine air masses with respect to the wind direction. Indeed, the variation in wind direction is usually accompanied by changes of the atmospheric aerosol characteristics, [26] with potential different interactions with the virus. Thus, in coastal areas, aerosol concentrations result from the complex mixing between particles produced by natural processes of continental and marine origins and particles of anthropogenic origin issued from urban and industrial activities. Among them, the sea-spray aerosols generated at the air–sea interface by wave breaking represent a major component of the natural aerosol mass [27–30]. The generation of sea-spray is due to two major mechanisms: the bubble-mediated production of jet and film droplets from breaking waves [31] effective at wind speeds from 4 ms^{-1} and up, and the production of spume droplets torn directly from wave crests by strong turbulence [32] effective at wind speeds in excess of 10–12 ms^{-1}. Additional aerosols are produced over the ocean's surface from secondary processes issued from the gaseous dimethyl sulfide (DMS) released from surface waters (e.g., Bates et al. [33]). These primary

and secondary marine aerosol production processes result in particles carrying widely in number and size, i.e., from less than 0.01 μm to about 500 μm [34].

In this paper, we focus on the influence of the maritime air masses on the SARS-CoV-2 propagation because it has been noted that the number of deaths in the French hospitals represents less than 15% of the total in regions with a maritime facade normalized to the population density (French Ministry of Health, 2020). It should be noted that a maritime character is not systematic for air masses over coastal areas. For example, Piazzola et al. [35] found that for low wind speeds air masses were strongly impacted by pollution on the French Mediterranean coast, and analogous situations were detected by Massabo' et al. [36] over the coastal zone of the Northern Adriatic Sea. Maritime conditions occur over coastal areas during onshore wind episodes with high velocity and long fetch above the sea. Among the maritime air mass properties, we point out the role of sea-spray aerosols and humidity in the lower atmospheric layer for their influence on the virus contamination. In this paper, we focus only on the March–April period, which corresponds to the French lockdown that contributed to reduce the influence of the human social behavior. Figure 1 shows the normalized number (per 100.000 residents) of deaths due to COVID-19 by department in France from March to July 2020 (i.e., during the first outbreak). The COVID-19 effects tended to be larger in the inner areas than in the areas subject to marine influence. This called for a study of the contamination rate of specific geographic areas with respect to the meteorological conditions and the corresponding air mass properties in order to better understand the role of sea spray in the virus propagation. To this end, we have compared two distinct French departments. It should be noted that important regional variations were recently observed in France in terms of the occurrence of new emerging virus variants (Haim-Boukobza et al. [37]), which could in principle modify the virus epidemiology.

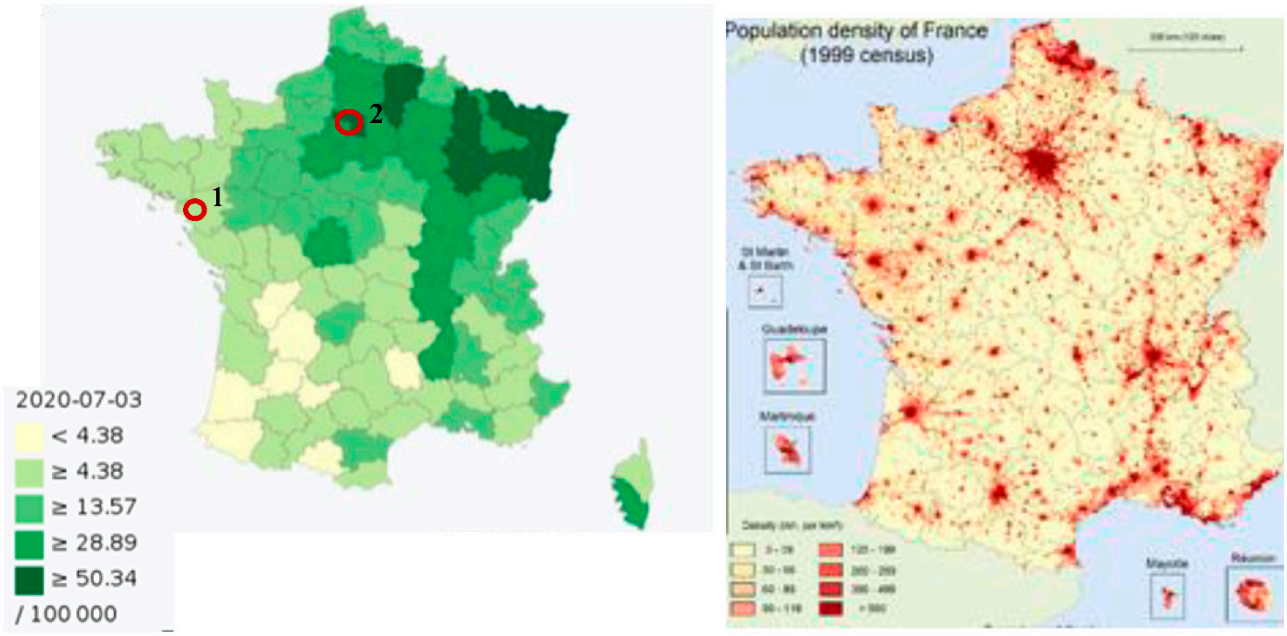

Figure 1. (**Left**): Number of deaths per 100000 residents by French departments. The circles denote the capital cities of the regions investigated: 1 = Nantes, 2 = Paris. (**Right**): population density of France. Images modified from https://en.wikipedia.org/wiki/COVID-19_pandemic_in_France (accessed on 19 February 2021) and https://en.wikipedia.org/wiki/Demographics_of_France (accessed on 19 February 2021).

The investigated pair is constituted by one coastal and one continental location. The continental French location is the Paris department, which was identified as a cluster for the pandemic with an excess in hospitalizations and deaths. This is compared to the trend of the contamination in the Loire-Atlantique department, a geographical area around Nantes, which is the largest and more industrialized city of the western part of France. This latter

one was spared by the virus in the beginning of the pandemic, but then knew a sudden increase in the contamination cases after the beginning of the confinement period, which was decided by the French government in the middle of March (i.e., the 17th). As outlined above, the geosocial factors—like population density, demographic and socio-economic structure, etc.—that can be relevant for COVID-19 outcomes and as potential confounding factors (e.g., Wu et al. [3]; Sobral et al. [38]) are reasonably similar in the two cities. To investigate if the aerosol properties can play a role in these differences between coastal and continental regions, we have analyzed the aerosol and meteorological data for every study area using ground-based measurements. In particular, the AERONET data allowed a survey of the aerosol properties, as optical depth (AOD) and Angstrom exponent in the selected locations during the spring 2020 COVID-19 outbreak. The present results are in favor of an influence of the maritime air-masses on the limitations of the virus impact via the role of the sea-spray and atmospheric humidity.

2. Field Sites and General Characterization of the Study Areas

We study both the meteorological characteristics and aerosol properties of two different specific geographical areas located in France. Our analysis focuses on the region around the city of Nantes, located in the French Atlantic shoreline, south of Brittany, and the inland Paris department (Figure 1).

The two French cities are both densely populated, characterized by large amounts of car traffic and surrounded by industrialized areas. However, the Atlantic shoreline near Nantes, as in the other French western regions, is most of the time under marine air masses' influence, while the capital city is quite constantly polluted [39]. In coastal areas, the wind direction is the first parameter to consider in our analysis, since changes in the wind direction may result in transport from different aerosol source regions. We will then study two particular types of meteorological conditions that often occur in the coastal area, offshore winds (which travel from land to the sea) and onshore winds (from the sea to the shore), which correspond to marine air mass conditions. Figure 2 shows the normalized number of deaths recorded in the Paris and Loire-Atlantique departments from March to May 2020, data publicly available from the official government website (https://www.gouvernement.fr/info-coronavirus/carte-et-donnees, accessed on 19 February 2021).

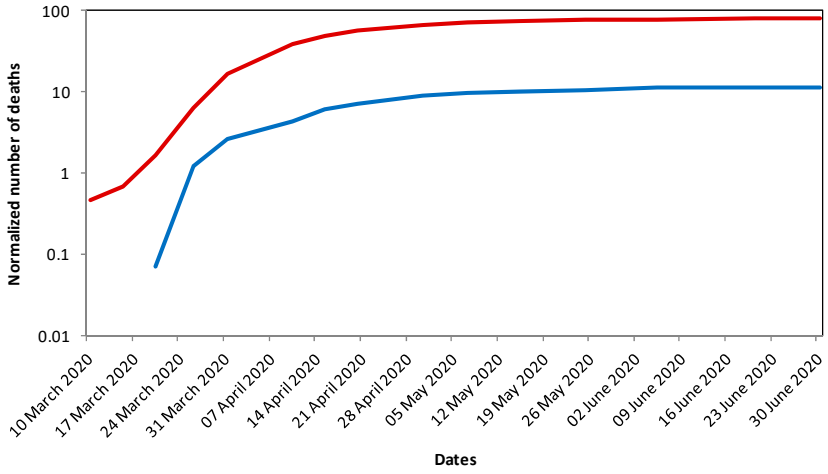

Figure 2. Number of deaths for COVID-19 per 100,000 residents by department in Paris (red line) and Loire-Atlantique (blue line). See https://www.gouvernement.fr/info-coronavirus/carte-et-donnees (accessed on 19 February 2021).

The population density of the Paris department is greater than that of Loire-Atlantique, but due to the fact that in the latter the majority of population is located in the city of Nantes (Figure 1) we believe that the comparison is not compromised by this confounding factor. We note a factor of about eight between the two French regions in the cumulative

results. In particular, in the beginning of March, a few hundred contamination cases were already reported in Paris, whereas only a few cases were detected in the Nantes region. Then, a sudden increase in the COVID-19 cases was recorded in the Nantes area at the end of March. In this paper, we propose to investigate the reasons of this behavior in terms of the mesoscale atmospheric transport.

3. Meteorological Conditions and Air Mass Properties

Aerosol dynamics are strongly dependent on the meteorological conditions [40]. As outlined above, the maritime air mass character is provided by an onshore wind direction with high velocity. To observe the respective contribution of both the onshore and the offshore winds, the wind rose of the wind direction recorded in Le Croisic in the period March–April 2020 is reported in Figure 3. We can see that high wind speed episodes largely correspond to the northwest and west directions, i.e., the onshore winds in the study area. This deals with the lower number of contaminations observed in Brittany (even in the second wave occurring in 2021).

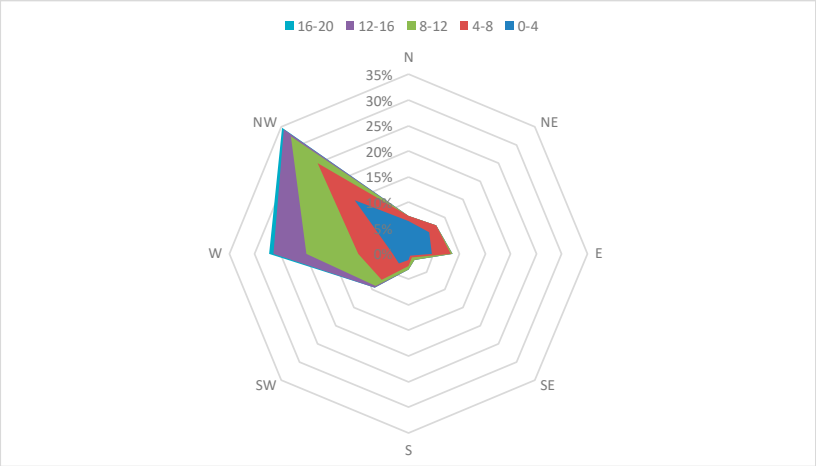

Figure 3. Wind rose recorded in Le Croisic in March April 2020. The wind speed intervals encountered during the campaign are reported above the graphic.

In addition, Figure 4 reports the temporal survey of both the wind speed and the direction measured in the period March–April 2020 in the coastal station—the SEM-REV site for multi-technology offshore testing—located in Le Croisic, twenty kilometers from Nantes near to the Atlantic shoreline (Figure 4a,b) and in the center of Paris (Figure 4b).

Figure 4a exhibits two distinct periods: until the end of March, it shows that the wind comes from western to south-western directions resulting in the transport of marine air masses in the study area, then the dominant wind system clearly comes from east. In addition, we can note that, in this first period, high wind speed episodes from the onshore direction are frequent, inducing both the production and transport of sea-spray aerosols [26]. Furthermore, such maritime conditions have also caused few rainy episodes (data not shown). As outlined above, after about one month of the purely marine system, Figure 4a shows that the wind direction turns east on the Atlantic shoreline. During this second period, the wind then keeps its direction for more than three weeks with rather low wind speeds. It should be noted that low wind speeds do not allow both the production of sea-spray at the air–sea interface and also an efficient atmospheric mixing (e.g., Piazzola and Despiau [26]). Indeed, the western part of France was first exposed to a long marine wind system, followed by anthropogenized air masses coming from the industrial region of Paris and its suburb. The decrease in the wind speed and the change in wind direction exhibited in Figure 4a at the end of March in Nantes seem to be well-correlated with the increase in the COVID-19 casualties, as noted in Figure 2.

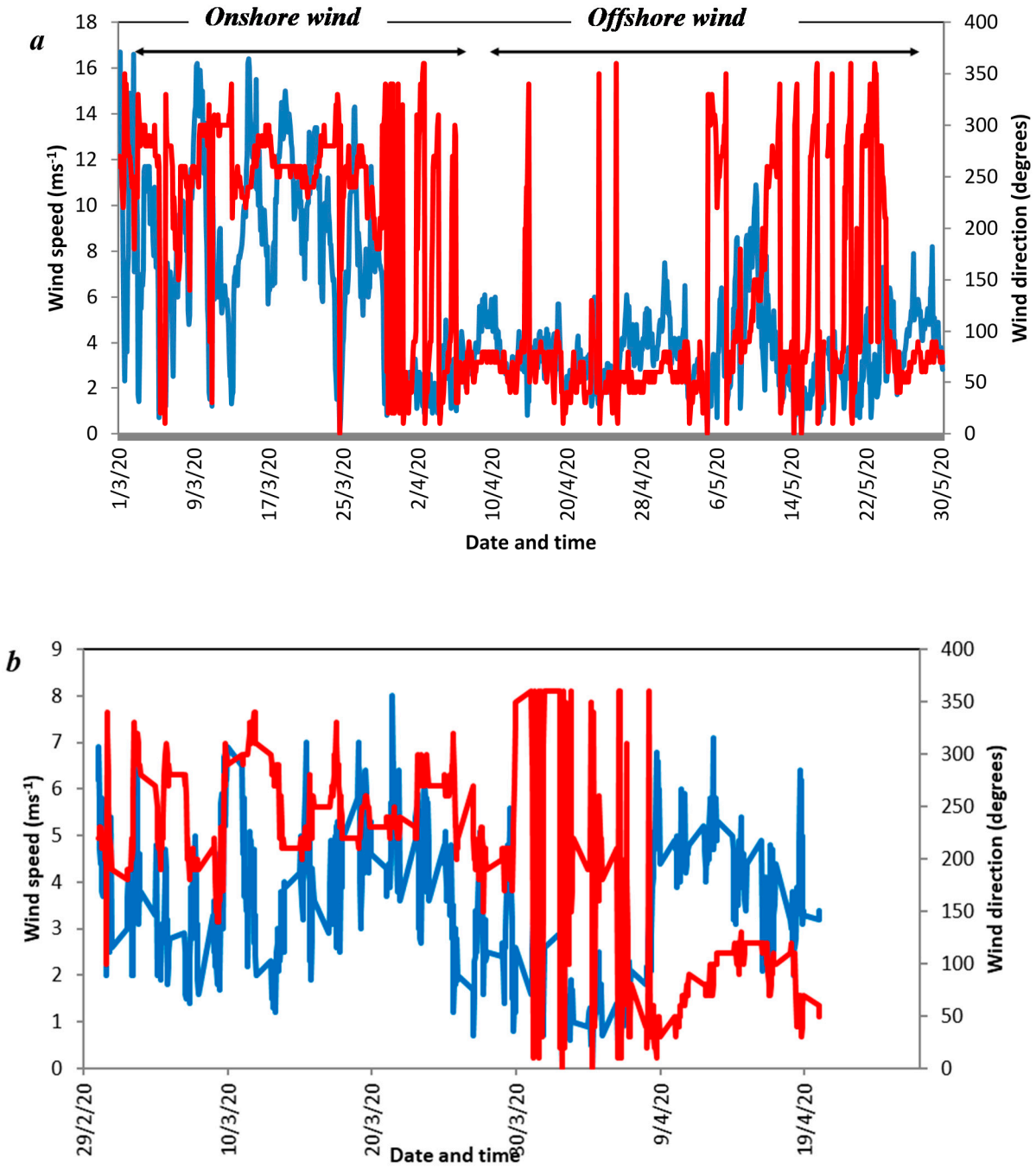

Figure 4. Time series of both the wind speed (the blue line) and direction (the red line) over March, and April 2020 in (**a**) the SEM-REV station located in Le Croisic near Nantes and (**b**) at the station of the Montsouris park in Paris. Above the Figure 4a is reported the onshore and offshore wind episodes that occur in the coastal site.

Figure 4b shows that Paris was exposed to east and southeast winds, which deal with land and urbanized influence. The wind speed rarely exceeded 6 ms^{-1} in the study period, which does not permit the strong turbulent dispersion of the atmospheric aerosols. However, there were therefore more opportunities for the wind to blow above the industrialized areas, as will be confirmed from the air mass properties (see below).

For each meteorological period presented in Figure 4, we have studied the properties of the corresponding air masses using numerical calculations of the air mass back-trajectories issued from the NOAA HYSPLIT model [41,42]. Figure 5 reports air mass back-trajectories from the French Atlantic shoreline for March 2020. As outlined above, it confirms that

western winds recorded until the end of March (see Figure 4a) deal with marine air mass coming from the open Atlantic Ocean. The first half of March probably allows the transport of sea-spray aerosols in the low atmosphere in the Nantes region. In contrast, after a short transition period, the air mass back-trajectories calculated for the eastern wind period, occurring in the second half of March, indicate the atmospheric transport to the Nantes region of the anthropogenic air masses coming from Paris.

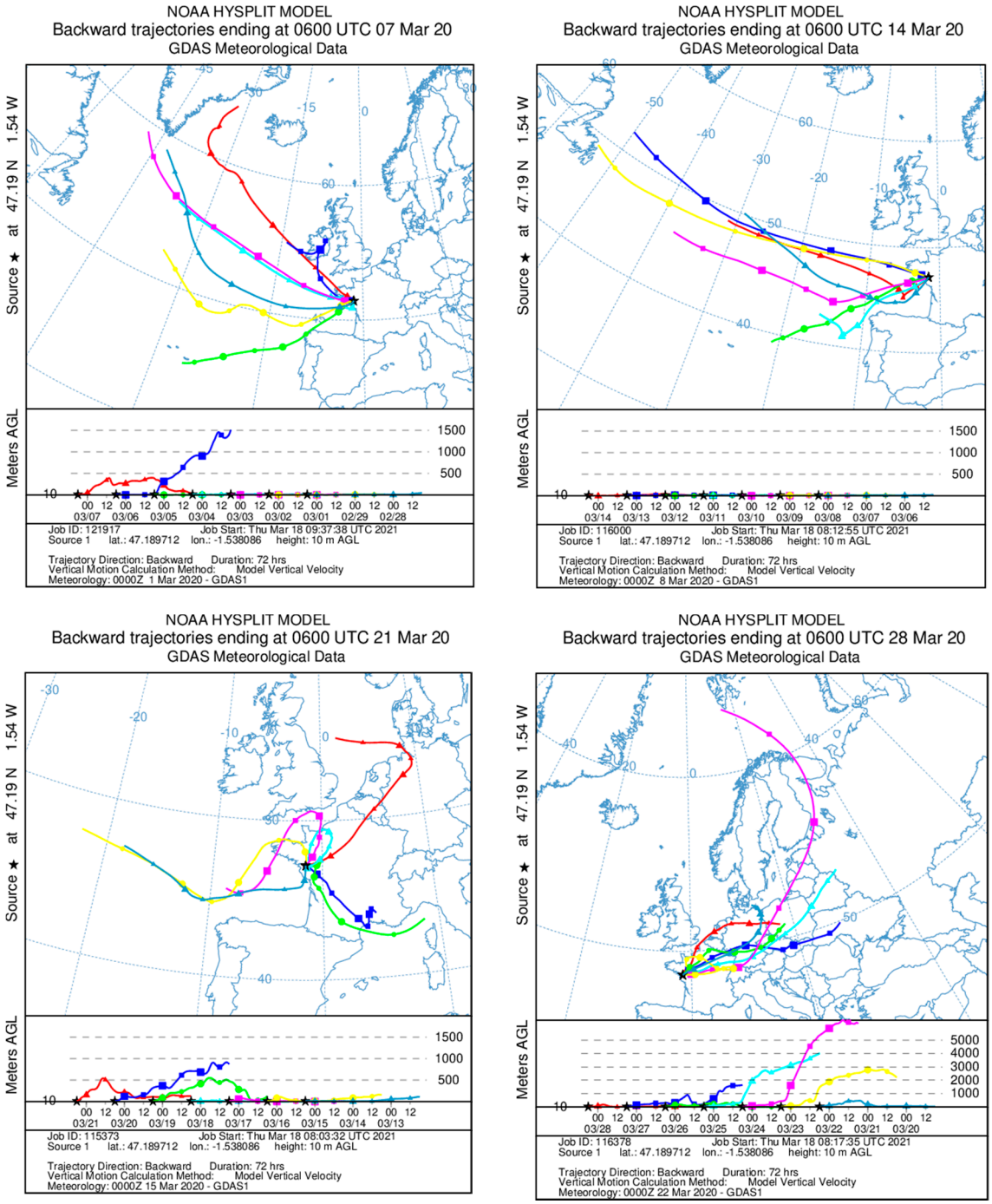

Figure 5. Calculated air mass back-trajectories in Nantes (French Atlantic shoreline) for March 2020.

Figure 6 presents the numerical calculations of the air mass back-trajectories in Paris for March 2020. According to Figure 6, we see that, in the second half of March, the air masses transported above the Paris area come essentially form the North-Western region,

which deals mainly with urbanized areas and probably transports anthropogenic aerosols. It should be noted that the western influence that occurs in the west coast of France can also affect the center of the country in Paris, but in this latter case, the wind then has the opportunity to cross the polluted regions and transport anthropogenic aerosols.

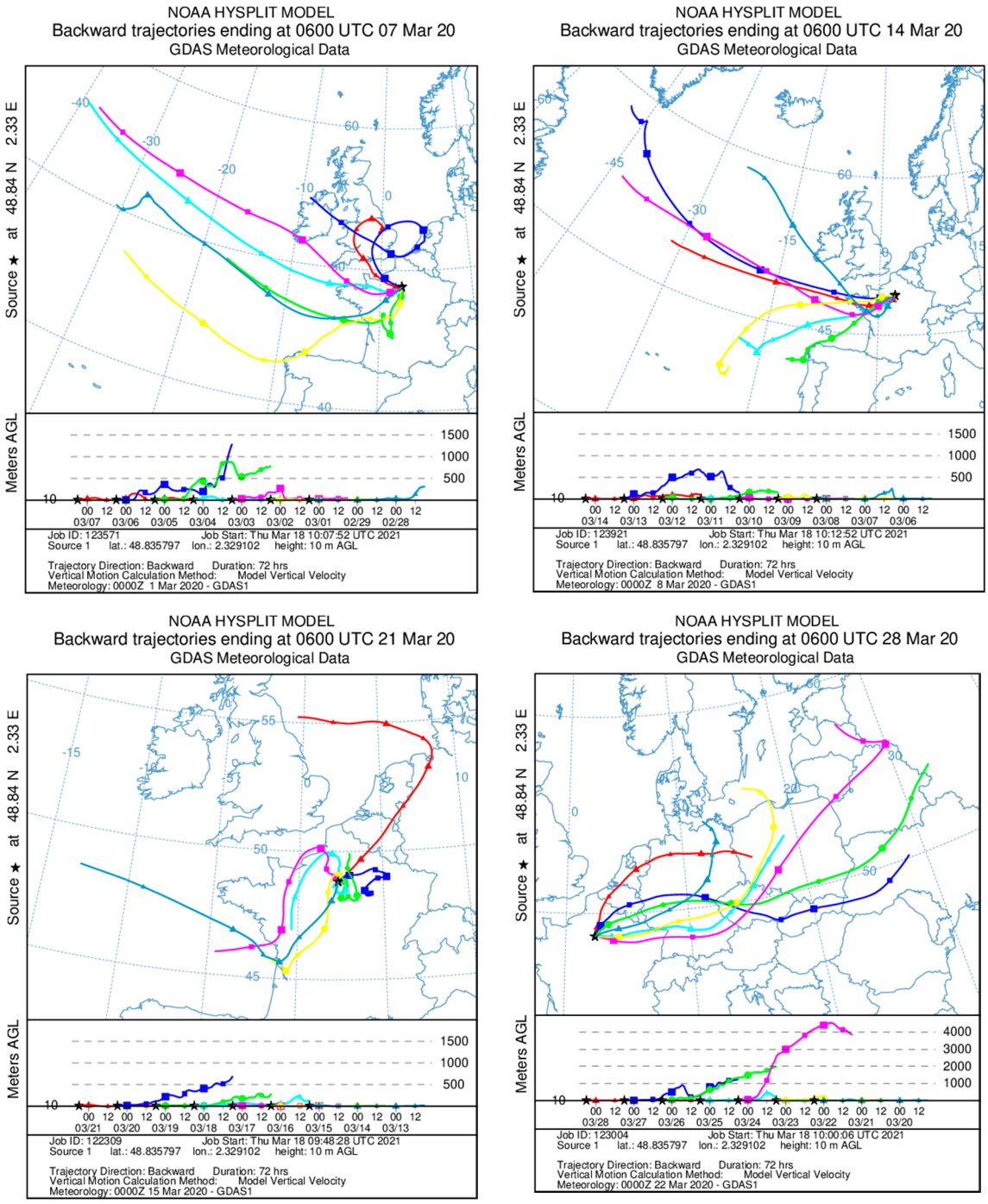

Figure 6. Calculated air mass back-trajectories in Paris for March 2020.

4. Survey of the Aerosol Properties

As noted in Section 3, combining the analysis of both the back-trajectory calculations and the wind conditions provide indirect information on the composition of the atmospheric aerosols transported in the regions investigated. To confirm our analysis and to study the influence of the air masses on the propagation of the COVID-19 during spring

2020, we also used the global data provided by the AERONET network. This is equipped with sun-photometers that provide information of the aerosol properties above the region considered. This gives the total (columnar) Aerosol Optical Depth (AOD), which is defined as the integral of the extinction coefficient, σ_{ext} along the air column from the ground to the top of the atmosphere:

$$AOD = \int_0^\infty \sigma_{ext}\, dz \quad (1)$$

where σ_{ext} is the extinction coefficient at altitude z.

The size distribution of the aerosols can be estimated from spectral AOD, typically from 440 nm to 870 nm. The AOD is then strongly related to the aerosol concentrations and properties on the atmospheric column. The AERONET program has provided high quality aerosol data for the past few decades over roughly 850 global stations. We selected suitable AERONET stations having a sufficiently large number of records per month. The number of observations per month basically depends on the seasonal daytime length, the station's location, the operational instrument status, the cloud disturbance, and the verification process of data quality. From Equation (1), we can readily calculate the AOD for each of the Sun–photometer bands at a specific wavelength λ, then by applying Angstrom's Law. The Angstrom coefficient, or exponent of the Angstrom diffusion α, reflects the dependence between the optical thickness of the aerosol and the wavelength. It is defined as the variation of the diffusion coefficient between two wavelengths such that:

$$\alpha = -\frac{ln[\tau_1]}{ln[\tau_2]} \quad (2)$$

where σ_1 and σ_2, the aerosol optical depth at wavelengths λ_1 and λ_2, respectively.

The Angstrom coefficient α, is then inversely related to the average particle size of the aerosol, i.e., the smaller the aerosols, the larger the coefficient. It is then a good indicator of the average distribution of the aerosol concentrations. As an example, values of α larger than 1 indicate the presence of small particles of anthropogenic or continental nature (such as smoke particles and sulfates, e.g., Saha et al. [43]), more particularly if the AOD value is low in the meantime (typically < 0.2). In contrast, small values of α (<1) indicate the presence of coarse mode particles such as desert dust and sea-spray (e.g., Dubovick et al. [44]). As for the marine particles generated by the breaking waves, they are generally large spherical aerosols, which also correspond to AOD (at 550 nm) roughly smaller than 0.2. In the maritime area, an industrial component may be accompanied by a variable marine component. If, like most of the time, the major contribution of marine aerosols is in the "coarse" mode, especially in the case of high relative humidity, we can still obtain a low Angstrom coefficient. As outlined above, the temporal behavior of both the Angstrom coefficient and the AOD can give an indication of the nature of the aerosols transported in the lower atmosphere. Moreover, by helping the analysis using the air mass back-trajectory calculations, the Angstrom parameter is enough in a first approach to characterize the size of the atmospheric particles.

In Figure 7 are reported the temporal variation of both the Angstrom coefficient and the AOD in Le Croisic over the period covering March 2020. We can note that Figure 7 exhibits two distinct portions whenever we consider data recorded before or after about the 15 March. During the first two weeks of March, the value of the Angstrom coefficient stays smaller than about 0.5, with an AOD smaller than 0.2, which indicates the presence of marine sea-spray in the coastal atmosphere. We can also observe in Figure 7, however, that a progressive increase in the Angstrom coefficient above the value of one occurs at the end of March, whereas the AOD increase in the meantime to vary around an average value of about 0.3 on the period. This sudden change in both the Angstrom coefficient and the AOD occurs at the date when the wind system changes, as shown in Figures 4a and 5. In turn, this indicates a change in the aerosol characteristics shifting from a prevalence of natural sea salt particles to anthropogenic ones.

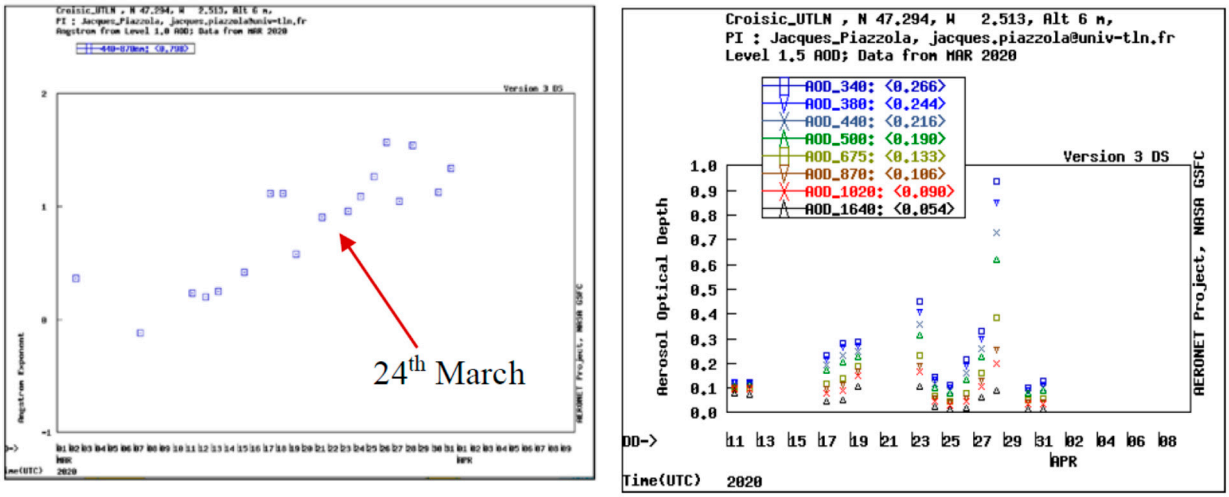

Figure 7. Temporal survey of the Angstrom coefficient (**left**) and the AOD (**right**) in Le Croisic (Nantes region) in March 2020. The arrow indicates the date of the occurrence of offshore wind conditions.

Figure 8 presents the temporal variation of both the Angstrom coefficient and the AOD in Paris along the period covering March 2020. The large Angstrom coefficient and small AOD observed in Figure 8 then confirm the presence of a substantial anthropogenic contribution in the atmospheric aerosols during March 2020. These aerosols are likely submicrometer particles of carbonaceous matter for a larger part, the major emission sources of soot particles in Europe being diesel engines and incomplete biomass burning. If we consider that the lockdown had started the 17th March in France, we assume that the major part of the atmospheric aerosols is of anthropogenic origin throughout the period. In particular, due to the low average temperature, the residential heating in Paris area had likely persisted during March 2020, while the traffic was almost stopped. The anthropogenic influence is shown to be nearly constant in Paris during the whole period. We can think that the emission of anthropogenic aerosols can be related to the continuous increase in COVID-19 contamination, as observed in the French capital city (see Figure 1). We could note that the Angstrom coefficient is positively correlated with the number of contaminations.

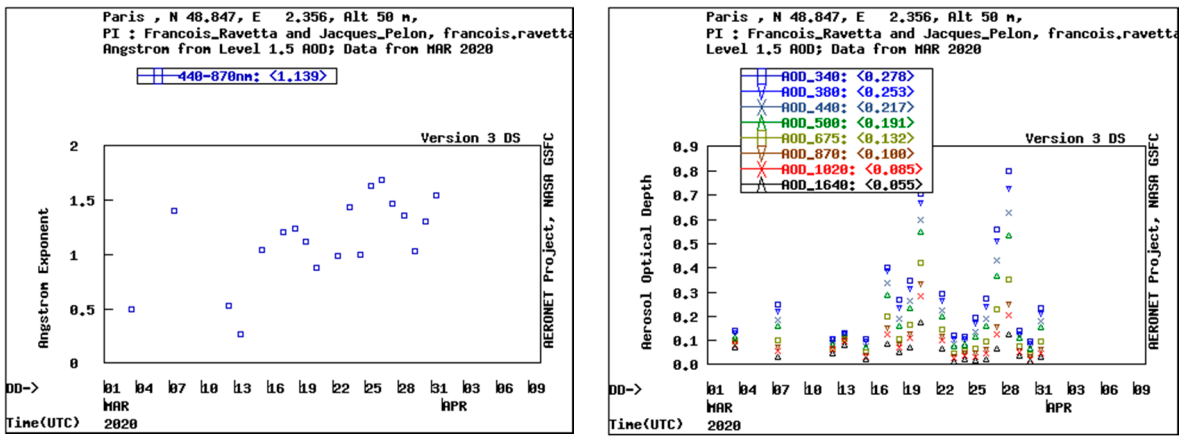

Figure 8. Temporal survey of the Angstrom coefficient (**left**) and the AOD (**right**) in Paris in March 2020.

5. Discussion

The transmission of SARS-CoV-2 by aerosols emitted from the human respiratory system and its viability have been supported by several recent studies [45–47]. Nevertheless, the whole set of parameters influencing its atmospheric propagation and their role are

poorly understood [48–50]. It is often a specific combination of them, characterizing specific atmospheric air masses, that leads to the enhanced incidence of infectious diseases [51]. The aim of this work was to study the environmental conditions and the role of atmospheric aerosols on COVID-19 contamination. To this end, we have compared two regions experiencing different atmospheric air masses and with different COVID-19 contamination rates. This work has implications on contamination because of both the indirect and direct effects of aerosols. Concerning direct effects, the potential risk of airborne indoor transmission has been demonstrated (e.g., Birnir [14]), and the indoor air environment is a mixing of specific indoor components emitted by indoor sources and outdoor air, including outdoor aerosol particles, that penetrates indoors [12,13].

The meteorological conditions near the coastal city of Nantes exhibit two distinct periods, which exactly correspond to an abrupt change in aerosol properties as indicated by the temporal behavior of both the Angstrom and the AOD during the same period (Figure 7). This also corresponds to a net increase in the COVID-19 cases in this western part of France observed in the second half of March (Figure 2). After two weeks, changes in the wind systems (Figure 4a), i.e., from onshore to offshore winds, induced a return of air mass conditions to a maritime character, and hence, a lower slope of the contamination cases was noted from the end of April.

In the meantime, continental sites such as the Paris region stay under influence of anthropogenic air masses for most of the time. The anthropogenic character of aerosols transported above the location is also confirmed by the study of the Angstrom coefficient, which attests the presence of a substantial anthropogenic contribution in the atmospheric aerosols during March 2020. In agreement with Isaia et al. [52] polluted aerosols can be hypothesized.

We hypothesize that the lifetime and viability of the virus in the atmosphere depends also on its ability to coagulate with aerosols. Coagulation is a phenomenon corresponding to the shock between two particles, which remain linked to form one particle. Coagulation is conditioned by the Brownian agitation of the air which takes into consideration the cross section of the particle and the collision probability of two particles. It can be expressed as the transverse area that the incident particle must hit in order for a collision to occur. According to the coagulation coefficient K, we can show (e.g., Fuchs, [53]) that the most rapid coagulation concerns particles of size about 0.1 μm, which corresponds to the diameter of the SARS-CoV-2 particle. Coagulation then acts a source and a sink for particles in the 0.02–0.15 μm size range [54]. Dusek et al. [55] suggest that size is the key parameter for the cloud-nucleating ability of aerosol particles, more than their composition. Figure 9 reports an example of the aerosol size distributions typical of the coastal zone issued from measurements conducted on the island of Porquerolles by Van Eijk et al. [34] As shown in Figure 9, the aerosol concentration dN/dr can be fitted by the sum of five lognormal functions centered on radii of 0.01, 0.03, 0.24, 2 and 10 μm. We can see that if the lower size of atmospheric particles can be small as 10 nm, sea salt mainly deals with supermicrometer aerosols with sizes up to 50 μm. The submicronic particles mainly deal with anthropogenic aerosols. In urban atmosphere, the anthropogenic particles, such as carbonaceous particles, present in the atmosphere have sizes close to the diameter of the virus particle and hence, can allow its transport through the coagulation processes. This supports the hypothesis that the atmospheric transport of the virus is favored by polluted aerosols.

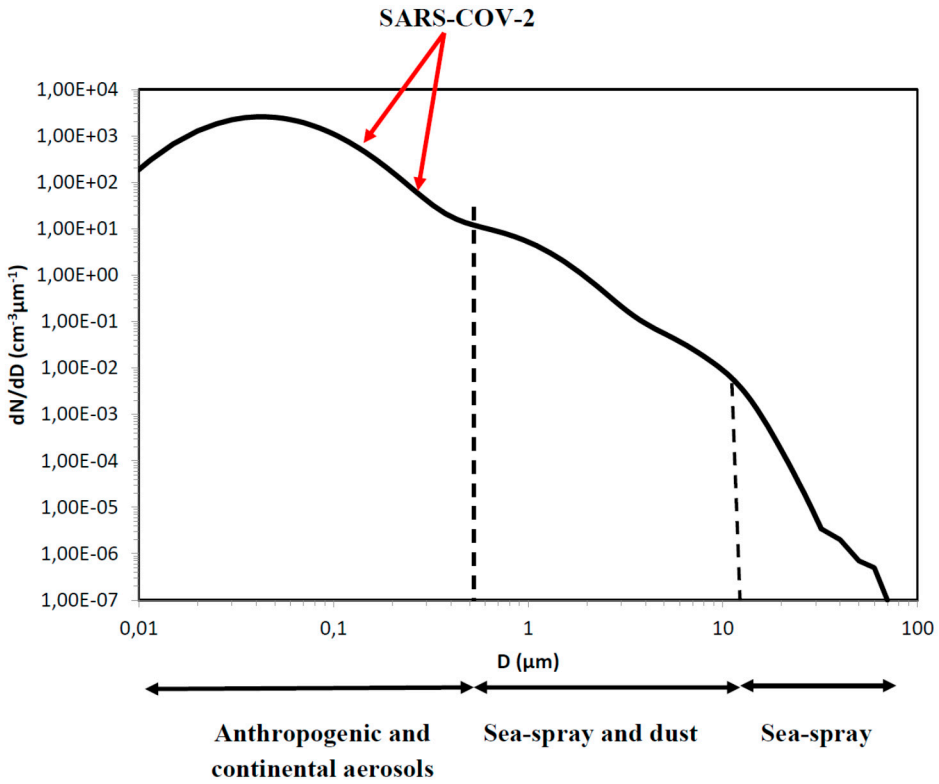

Figure 9. An example of aerosol size distributions typical of the coastal zone issued from measurements conducted on the island of Porquerolles by Van Eijk et al. (2011). As shown, the aerosol concentration *dN/dr* can be fitted by the sum of five lognormal functions centered on radii of 0.01, 0.03, 0.24, 2 and 10 µm. (the black line). The dashed lines indicate the size intervals dealing with the different aerosol sources found in the coastal zone. The arrows indicate the expected size of SARS-CoV2 (around 100 nm).

In addition, anthropogenic aerosols will increase the sensitivity of fragile people to develop virus disease, [56] worsening the number of cases and fatalities. In this latter case, we suspect a strong role of carbonaceous anthropogenic aerosols emissions, which allow better atmospheric transport of the SARS-CoV-2 through their fractal aspect by facilitating the aggregation of some viruses on it. The major emission sources of soot particles in large parts of Europe are diesel engines and incomplete biomass burning. An abundant constituent in atmospheric aerosols is carbonaceous matter (CM), which is composed of black carbon (BC) and organic carbon (OC). BC is commonly referred to as soot, whose submicrometer size and fractal morphologies may favor efficient interactions with the virus and its coagulation upon the particle. As the confinement had started on the 17th March in France, it suggests that the major part of the atmospheric aerosols is black carbon (BC) issued from wood burning emissions, in particular if we consider that wood heating (residential heating) in Paris still persisted during March 2020, whereas traffic jams were almost stopped. It should be noted that another continental example can be found in the literature, which had approximately the same behavior as Paris (see Conticini et al. [19]), with a similar polluted character of the air masses transported above the city during the period. In contrast, in coastal areas, the contamination rate can be low, reflecting a potential consequence of viral activity inactivation by maritime air masses. In addition to the size, the morphology of the aerosols can also affect the coagulation process. The morphology of sea salt is cubic and flat whereas the soot has a complex form, as shown in Figure 10, which reports scanning electron microcopy (SEM) images of aerosol samples acquired using a Dekati impactor (e.g., Piazzola et al. [35]) on the Mediterranean island of Porquerolles [57]. The fractal aspect of the carbon particles could indeed facilitate the aggregation of some viruses on it. It should be noted that Figure 10 shows pictures of samples taken on a filter

on which aerosols are mixed, but it is not demonstrated in the atmosphere. However, if an external mixing between sea salt and soot occurs in the atmosphere, we can imagine that the virus aggregate on the soot could be affected by the humidity of the sea-spray aerosol. In particular, if we consider that high wind speed periods of marine winds induce increase in the ambient relative humidity [58]. The survivability of enveloped viruses, such as SARS-CoV-2, seems to be linked to temperature and humidity in a complex and nonmonotonic manner [5,59]. As an example, Ma et al. [60] and Wu et al. [3] provided preliminary evidence that the COVID-19 pandemic may be partially suppressed with temperature and humidity increases.

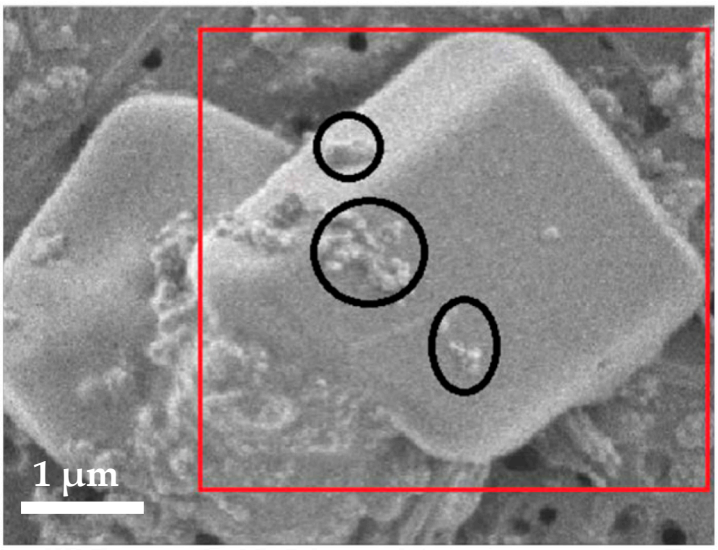

Figure 10. SEM image of a mixing sea-spray-soot as sampled on the Mediterranean coast using a Dekati impactor. The red square denotes a salt crystal, while the black circles show soot. The photograph is issued from aerosol samples acquired on the island of Porquerolles during the MATRAC experiments (Piazzola et al., 2020) [61].

Following the coagulation, atmospheric reaction between virus and sea-spray is also possible since sea-spray is known to react with various atmospheric gas and aerosol components (see Piazzola et al. [62] as an example). Sea salt aerosols are humid particles mainly constituted of sodium chloride (NaCl). Salt-contained aerosols can act as inhibiting factors for the virus activity. For instance, Quan et al. [63] demonstrated that viruses captured on salt-coated filters exhibited rapid infectivity loss compared to a gradual decrease on bare filters. Sea-spray aerosols constitute strongly hygroscopic particles that instantaneously answer the humidity variations by varying in size [64]. The increase in relative humidity induces an enhancement of the sea-spray sizes through the increase in the amount of the water vapor around the droplet. The radius of sea salt particles at 100% relative humidity is twice that at a relative humidity of 80% [65]. The injection of a large volume of sea-spray particles in the atmosphere results in a larger ambient humidity in the lower atmosphere through aerosol evaporation. For onshore winds, high wind speeds are positively correlated with high relative humidity, as shown in Figure 11, which presents the variation of the relative humidity when the wind speed of a marine direction increases in the case of a coastal marine air mass episode (this is not systematic for offshore winds) [26]. Chan et al. [66] show that a high relative humidity (>95%) combined with a high temperature (38 °C) led to a 0.25~2 loss of titer in 24 hours for the SARS coronavirus. Viral particles coagulated with sea-spray are surrounded by a very humid environment and it can be hypothesized that, in the marine atmosphere where a lot of large humid particles are present, virus infectivity will decrease rapidly. In contrast, even though humidity can be high in urbanized areas, the anthropogenic aerosols are mostly not hygroscopic and hence do not affect the infectivity of the virus. Kanji et al. [67] note that freshly emitted

soot is hydrophobic. In addition, field observations show that, most of the time, small atmospheric particles do not answer to humidity (Dusek et al. [55]).

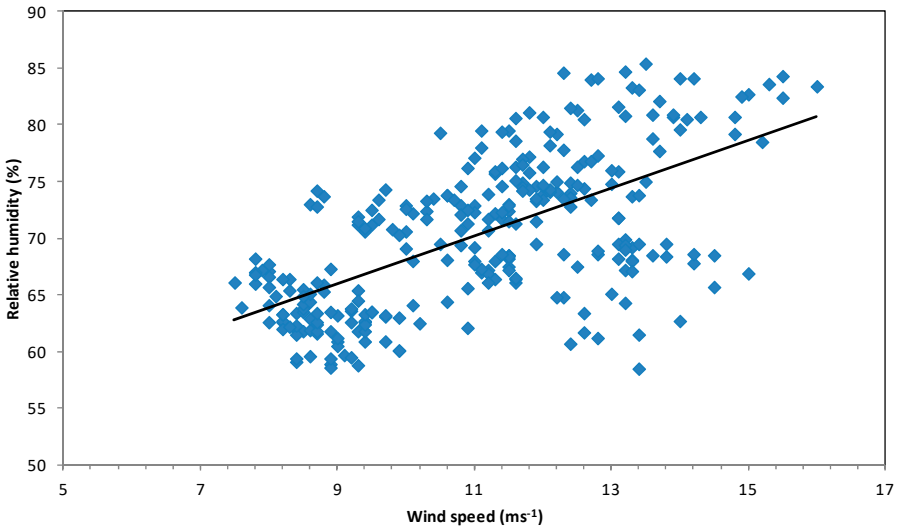

Figure 11. Variation of the relative humidity versus wind speed for an onshore wind direction (marine air mass episode). The data were recorded on the island of Porquerolles by Piazzola (personal communication). The black line fits the data.

We therefore propose that the coagulation of the SARS-Cov-2 with anthropogenic aerosols protects the virus particle from ambient humidity and preserves its infectivity, whereas the coagulation with humid sea-spray rapidly inhibits its activity, in particular through the reaction of the salt with the virus. On the basis of our results, a main trend is emerging: the risk of ambient contamination by the SARS-CoV-2 is less important for locations under marine air masses' influence and more particularly when the wind speed is frequently strong enough to allow the atmospheric transport of freshly produced sea-spray particles. In the coastal area that we considered, the contamination rate is low, reflecting a potential consequence of viral activity reduction by maritime air masses. This is not, however, systematic for all maritime regions, since few of them are under the influence of offshore winds, such as the Mistral for the Western Mediterranean coast of France (near Marseille), most of the time. Laboratory work is in progress to confirm our hypothesis on the role of the sea-spray aerosols on the survival of the SARS-Cov-2 virus in the marine atmosphere.

6. Conclusions

The aim of this paper was to study the contamination rate of both a continental and a coastal geographic area in France with respect to the meteorological conditions and the corresponding air mass properties. The regions investigated in this paper were very different in terms of the number of contamination cases. Comparing only two regions is undeniably a limit of the present study. Nevertheless, our results indicate that the risk of contamination by the COVID-19 was less important for the location under marine air masses' influence and more particularly when the wind speed was frequently strong enough to allow the atmospheric transport of freshly produced sea-spray particles. This reflects a potential consequence of the viral activity reduction by the maritime air masses. In view of the systematically lower number of cases in this maritime area, we hypothesized an impact of the marine aerosol.

Our results suggest that the marine air mass influence could have an effect on the SARS-CoV-2 through both the morphology and/or the hygroscopic character of sea-spray aerosols in the lower atmosphere, as well as a possible reaction with the salt onto the spray particles [63]. It is then possible that marine episodes tend to decrease virus infectivity

by the coagulation of the virus with sea-spray aerosols. In contrast, in polluted areas, the facilitated coagulation processes with nonhygroscopic anthropogenic aerosols makes the virus more infectious over larger periods, more particularly indoors where the virus concentration is more relevant. This is in addition to the combination with the capability of the anthropogenic aerosols to increase the sensitivity of fragile people to develop viruses [56].

Further studies, also in other maritime areas around the world, will be required to assess the robustness of this approach for a better prediction of the SARS-COV-2 propagation and activity according to the trajectory and the nature of the air masses. In addition, it should be noted that the recent occurrence of virus variants, observed in France with different frequency across regions (Haim-Boukobza et al. [37]), is a complicating factor. Work is currently in progress to confirm our hypothesis on the role of the sea-spray aerosols on the survival of the SARS-CoV-2 virus in marine atmosphere.

Author Contributions: Conceptualization, J.P., E.C. and C.D.; methodology, J.P., W.B. and E.C., formal analysis, J.P., W.B. and C.D.; resources, C.Y.; data curation, J.P. and C.Y.; writing—original draft preparation, J.P.; writing—review and editing, J.P., E.C. and P.P.; supervision, J.P.; project administration, J.P.; funding acquisition, J.P. All authors have read and agreed to the published version of the manuscript.

Funding: This work was sponsored by ANR-ASTRID under contract ANR-18-ASTR-0002.

Institutional Review Board Statement: Not applicable.

Informed Consent Statement: Not applicable.

Data Availability Statement: Not applicable.

Acknowledgments: This work was sponsored by ANR-ASTRID under contract ANR-18-ASTR-0002. The authors wish to thank Antoine Bertholon, Arnaud Blangy, Yves Perignon of the SEM-RV and Tathy Missamou for their help to the experimental effort in Le Croisic. Prs. François Ravetta and Jacques Pelon are gratefully acknowledged for the use of the AERONET data. The authors gratefully acknowledge the NOAA Air Resources Laboratory (ARL) for the provision of the HYSPLIT transport and dispersion model and/or READY website (http://www.ready.noaa.gov, accessed on 19 February 2021) used in this publication. A special thanks to Olivier Grauby for the SEM photographs.

Conflicts of Interest: The authors declare no conflict of interest.

References

1. Geller, C.; Varbanov, M.; Duval, R. Human coronaviruses: Insights into environmental resistance and its influence on the development of new antiseptic strategies. *Viruses* **2012**, *4*, 3044–3068. [CrossRef]
2. Jia, J.S.; Lu, X.; Yuan, Y.; Xu, G.; Jia, J.; Christakis, N.A. Population flow drives spatio-temporal distribution of COVID-19 in China. *Nature* **2020**, *582*, 389–394. [CrossRef] [PubMed]
3. Bi, Q.; Wu, Y.; Mei, S.; Ye, C.; Zou, X.; Zhang, Z.; Liu, X.; Wei, L.; Truelove, S.A.; Zhang, T.; et al. Epidemiology and transmission of COVID-19 in 391 cases and 1286 of their close contacts in Shenzhen, China: A retrospective cohort study. *Lancet Infect. Dis.* **2020**, *20*, 911–919. [CrossRef]
4. Wu, Y.; Jing, W.; Liu, J.; Ma, Q.; Yuan, J.; Wang, Y.; Du, M.; Liu, M. Effects of temperature and humidity on the daily new cases and new deaths of COVID-19 in 166 countries. *Sci. Total Environ.* **2020**, *729*, 139051. [CrossRef]
5. Srivastava, A. COVID-19 and air pollution and meteorology-an intricate relationship: A review. *Chemosphere* **2021**, *263*, 128297. [CrossRef]
6. Meselson, M. Droplets and aerosols in the transmission of SARS-CoV-2. *N. Engl. J. Med.* **2020**, *382*, 2063. [CrossRef]
7. Rabaan, A.A.; Al-Ahmed, S.H.; Al-Malkey, M.K.; Alsubki, R.A.; Ezzikouri, S.; Al-Habab, F.H.; Sah, R.; Al Mutair, A.; Alhumaid, S.; Al-Tawfiq, J.A.; et al. Airborne transmission of SARS-CoV-2 is the dominant route of transmission: Droplets and aerosols. *Infez. Med.* **2021**, *29*, 10–19, PMID: 33664169. [PubMed]
8. Balachandar, S.; Zaleski, S.; Soldati, A.; Ahmadi, G.; Bourouiba, L. Host-to-host airborne transmission as a multiphase flow problem for science-based social distance guidelines. *Int. J. Multiph. Flow* **2020**, *132*, 103439. [CrossRef]
9. Da Silva, P.G.; Nascimento, M.S.J.; Soares, R.R.G.; Sousa, S.I.V.; Mesquita, J.R. Airborne spread of infectious SARS-CoV-2: Moving forward using lessons from SARS-CoV and MERS-CoV. *Sci. Total Environ.* **2020**, *764*, 142802. [CrossRef]
10. Belosi, F.; Conte, M.; Gianelle, V.; Santachiara, G.; Contini, D. On the concentration of SARS-CoV-2 in outdoor air and the interaction with pre-existing atmospheric particles. *Environ. Res.* **2021**, *193*, 110603. [CrossRef]
11. Morawska, L.; Tang, J.W.; Bahnfleth, W.; Bluyssen, P.M.; Boerstra, A.; Buonanno, G.; Cao, J.; Dancer, S.; Floto, A.; Franchimon, F.; et al. How can airborne transmission of COVID-19 indoors be minimised? *Environ. Int.* **2020**, *142*, 105832. [CrossRef]

12. Nwanaji-Enwerem, J.C.; Allen, J.G.; Beamer, P.I. Another invisible enemy indoors: COVID-19, human health, the home, and United States indoor air policy. *J. Expo. Sci. Environ. Epidemiol.* **2020**, *30*, 773–775. [CrossRef]
13. Tofful, L.; Perrino, C.; Canepari, S. Comparison study between indoor and outdoor chemical composition of PM2.5 in two Italian areas. *Atmosphere* **2020**, *11*, 368. [CrossRef]
14. Birnir, B. Ventilation and the SARS-CoV-2 Coronavirus analysis of outbreaks in a restaurant and on a bus in China, and at a call center in South Korea. *medRxiv* **2021**. preprint. [CrossRef]
15. Cacho, P.M.; Hernández, J.L.; López-Hoyos, M.; Martínez-Taboada, V.M. Can climatic factors explain the differences in COVID-19 incidence and severity across the Spanish regions?: An ecological study. *Environ. Health* **2020**, *19*, 106. [CrossRef]
16. Schwartz, J.; Dockery, D.W. Particulate air pollution and daily mortality in Steubenville, Ohio. *Am. J. Epidemiol.* **1992**, *135*, 12–19. [CrossRef]
17. Dockery, D.W.; Pope, C.A. Acute respiratory effects of particulate air pollution. *Annu. Rev. Public Health* **1994**, *15*, 107–132. [CrossRef]
18. European Environment Agency. *Air Quality in Europe; EEA Report No 10/2019*; Publications Office of the European Union: Luxembourg, 2019.
19. Conticini, E.; Frediani, B.; Caro, D. Can atmospheric pollution be considered a co-factor in extremely high level of SARS-CoV-2 lethality in Northern Italy? *Environ. Pollut.* **2020**, *261*, 114465. [CrossRef]
20. Pyankov, O.V.; Bodnev, S.A.; Pyankova, O.G.; Agranovskib, I.E. Survival of aerosolized coronavirus in the ambient air. *J. Aerosol Sci.* **2018**, *115*, 158–163. [CrossRef] [PubMed]
21. Setti, L.; Passarini, F.; de Gennaro, G.; Barbieri, P.; Pallavicini, A.; Ruscio, M.; Piscitelli, P.; Colao, A.; Miani, A. Searching for SARS-COV-2 on particulate matter: A possible early indicator of COVID-19 epidemic recurrence. *Int. J. Environ. Res. Public Health* **2020**, *17*, 2986. [CrossRef]
22. Contini, D.; Costabile, F. Does air pollution influence COVID-19 outbreaks? *Atmosphere* **2020**, *11*, 377. [CrossRef]
23. Pozzer, A.; Dominici, F.; Haines, A.; Witt, C.; Münzel, T.; Lelieveld, J. Regional and global contributions of air pollution to risk of death from COVID-19. *Cardiovasc. Res.* **2020**. [CrossRef]
24. Holben, B.N.; Eck, T.F.; Slutsker, I.; Tanre, D.; Buis, J.P.; Setzer, A.; Vermore, E.; Reagan, J.A.; Kaufman, Y.J.; Nakajima, T.; et al. AERONET—A federal instrument network and data archive for aerosol characterization. *Remote Sens. Environ.* **1998**, *66*, 1–16. [CrossRef]
25. Mallet, M.; Gomes, L.; Salmon, F.; Sellegri, K.; Pont, V.; Roger, J.C.; Piazzola, J. Calculation of key optical properties of the main anthropogenic aerosols over the Western French coastal Mediterranean Sea. *Atmos. Res.* **2011**, *101*, 396–411. [CrossRef]
26. Piazzola, J.; Despiau, S. Contribution of marine aerosols in the particle size distributions observed in Mediterranean coastal zone. *Atmos. Environ.* **1997**, *31*, 2991–3009. [CrossRef]
27. Andreae, M.O. Climate effects of changing atmospheric aerosol levels. In *World Survey of Climatology. Future Climate of the World*; Henderson-Sellers, A., Ed.; Elsevier: Amsterdam, The Netherlands, 1995; Volume 16, pp. 341–392.
28. Yoon, Y.J.; Ceburnis, D.; Cavalli, F.; Jourdan, O.; Putaud, J.P.; Facchini, M.C.; Decesari, S.; Fuzzi, S.; Sellegri, K.; Jennings, S.G.; et al. Seasonal characteristics of the physicochemical properties of North Atlantic marine atmospheric aerosols. *J. Geophys. Res.* **2007**, *112*, D04206. [CrossRef]
29. Mulcahy, J.P.; O'Dowd, C.D.; Jennings, S.G.; Ceburnis, D. Significant enhancement of aerosol optical depth in marine air under high wind conditions. *Geophys. Res. Lett.* **2008**, *35*, L16810. [CrossRef]
30. Piazzola, J.; Forget, P.; Lafon, C.; Despiau, S. Spatial variation of sea-spray fluxes over a Mediterranean coastal zone using a sea-state model. *Bound. Layer Meteorol.* **2009**, *132*, 167–183. [CrossRef]
31. Spiel, D.E. The sizes of jet drops produced by air bubbles bursting on sea- and fresh-water surfaces. *Tellus* **1994**, *46B*, 325–338. [CrossRef]
32. Veron, F. Ocean spray. *Annu. Rev. Fluid Mech.* **2015**, *47*, 507–538. [CrossRef]
33. Bates, T.S.; Kiene, R.P.; Wolfe, G.V.; Matrai, P.A.; Chavez, F.P.; Buck, K.R.; Blomquist, B.W.; Cuhel, R.L. The cycling of sulfur in surface seawater of the Northeast Pacific. *J. Geophys. Res.* **1994**, *99*, 7835–7843. [CrossRef]
34. Van Eijk, A.M.J.; Kusmierczyk-Michulec, J.T.; Piazzola, J. The Advanced Navy Aerosol Model (ANAM): Validation of small-particle modes. In *Atmospheric Optics IV: Turbulence and Propagation, Proceedings of the SPIE Optical Engineering + Applications, San Diego, CA, USA, 21–25 August 2011*; International Society for Optics and Photonics: Bellingham, WA, USA, 2011; Volume 8161. [CrossRef]
35. Piazzola, J.; Sellegri, K.; Bourcier, L.; Mallet, M.; Tedeschi, G.; Missamou, T. Physicochemical characteristics of aerosols measured in the spring time in the Mediterranean coastal zone. *Atmos. Environ.* **2012**, *54*, 545–556. [CrossRef]
36. Massabo', D.; Prati, P.; Canepa, E.; Bastianini, M.; van Eijk, A.M.J.; Missamou, T.; Piazzola, J. Characterization of carbonaceous aerosols over the Northern Adriatic Sea in the JERICO-NEXT project framework. *Atmos. Environ.* **2020**, *228*, 117449. [CrossRef]
37. Haim-Boukobza, S.; Roquebert, B.; Trombert-Paolantoni, S.; Lecorche, E.; Verdurme, L.; Foulongne, V.; Selinger, C.; Michalakis, Y.; Sofonea, M.T.; Alizon, S. Monitoring SARS-CoV-2 variants spread in France using specific RT-PCR testing. *medRxiv* **2021**. Preprint posted 23 February 2021. Available online: https://www.medrxiv.org/content/10.1101/2021.02.20.21251927v1.full (accessed on 19 February 2021).
38. Sobral, M.F.F.; Duarte, G.B.; da Penha Sobral, A.I.G.; Marinho, M.L.M.; de Souza Melo, A. Association between climate variables and global transmission of SARS-CoV-2. *Sci. Total Environ.* **2020**, *729*, 138997. [CrossRef] [PubMed]

39. Von der Weiden-Reinmüller, S.-L.; Drewnick, F.; Zhang, Q.J.; Freutel, F.; Beekmann, M.; Borrmann, S. Megacity emission plume characteristics in summer and winter investigated by mobile aerosol and trace gas measurements the Paris metropolitan area. *Atmos. Chem. Phys.* **2014**, *14*, 12931–12950. [CrossRef]
40. Fitzgerald, J.W. Marine aerosols: A review. *Atmos. Environ. Part A Gen. Top.* **1991**, *25*, 533–545. [CrossRef]
41. Rolph, G.; Stein, A.; Stunder, B. Real-time environmental applications and display sYstem: READY. *Environ. Model. Softw.* **2017**, *95*, 210–228. [CrossRef]
42. Stein, A.F.; Draxler, R.R.; Rolph, G.D.; Stunder, B.J.B.; Cohen, M.D.; Ngan, F. NOAA's HYSPLIT atmospheric transport and dispersion modeling system. *Bull. Am. Meteorol. Soc.* **2015**, *96*, 2059–2077. [CrossRef]
43. Saha, A.; Mallet, M.; Dubuisson, P.; Piazzola, J.; Despiau, S. One year measurements of aerosol optical properties over an urban coastal site: Effect on local direct radiative forcing. *Atmos. Res.* **2008**, *90*, 195–202. [CrossRef]
44. Dubovik, O.; Holben, B.N.; Eck, T.F.; Smirnov, A.; Kaufman, Y.J.; King, M.D.; Tanre, D.; Slutsker, I. Variability of ab-sorption and optical properties of key aerosol types observed inworldwide locations. *J. Atmos. Sci.* **2002**, *59*, 590–608. [CrossRef]
45. Guo, Z.-D.; Wang, Z.-Y.; Zhang, S.-F.; Li, X.; Li, L.; Li, C.; Cui, Y.; Fu, R.-B.; Dong, Y.-Z.; Chi, X.-Y.; et al. Aerosol and surface distribution of severe acute respiratory syndrome coronavirus 2 in hospital wards, Wuhan, China. (published online ahead of print April 10, 2020). *Emerg. Infect. Dis.* **2020**, *26*, 1586–1591. [CrossRef] [PubMed]
46. Van Doremalen, N.; Bushmaker, T.; Morris, D.H.; Holbrook, M.G.; Gamble, A.; Williamson, B.N.; Tamin, A.; Harcourt, J.L.; Thornburg, N.J.; Gerber, S.I.; et al. Aerosol and surface stability of SARS-CoV-2 as compared with SARS-CoV-1. *N. Engl. J. Med.* **2020**, *382*, 1564–1567. [CrossRef]
47. Chia, P.Y.; Coleman, K.K.; Tan, Y.K.; Ong, S.W.X.; Gum, M.; Lau, S.K.; Lim, L.X.; Lim, A.I.; Sutjipto, S.; Lee, P.H.; et al. Detection of air and surface contamination by SARS-CoV-2 in hospital rooms of infected patients. *Nat. Commun.* **2020**, *11*, 2800. [CrossRef] [PubMed]
48. Sagripanti, J.-L.; Lytle, C.D. Estimated Inactivation of Coronaviruses by solar radiation with special reference to COVID-19. *Photochem. Photobiol.* **2020**, *96*, 731–737. [CrossRef] [PubMed]
49. Schuit, M.; Ratnesar-Shumate, S.; Yolitz, J.; Williams, G.; Weaver, W.; Green, B.; Miller, D.; Krause, M.; Beck, K.; Wood, S.; et al. Airborne SARS-CoV-2 is rapidly inactivated by simulated sunlight. *J. Infect. Dis.* **2020**, *222*, 564–571. [CrossRef]
50. Ratnesar-Shumate, S.; Williams, G.; Green, B.; Krause, M.; Holland, B.; Wood, S.; Bohannon, J.; Boydston, J.; Freeburger, D.; Hooper, I.; et al. Simulated sunlight rapidly inactivates SARS-CoV-2 on surfaces. *J. Infect. Dis.* **2020**, *222*, 214–222. [CrossRef]
51. Hochman, A.; Alpert, P.; Negev, M.; Abdeen, Z.; Mohsen Abdeen, A.; Pinto, J.G.; Levine, H. The relationship between cyclonic weather regimes and seasonal influenza over the Eastern Mediterranean. *Sci. Total Environ.* **2021**, *750*, 141686. [CrossRef]
52. Isaia, G.; Diémoz, H.; Maluta, F.; Fountoulakis, I.; Ceccon, D.; di Sarra, A.; Facta, S.; Fedele, F.; Lorenzetto, G.; Siani, A.M.; et al. Does solar ultraviolet radiation play a role in COVID-19 infection and deaths? An environmental ecological study in Italy. *Sci. Total Environ.* **2020**. [CrossRef]
53. Fuchs, N.A. *The Mechanics of Aerosols*; Pergamon Press: Oxford, UK, 1964.
54. Raes, F.; Wilson, J.; van Dingen, R. Aerosol dynamics and it simplication for global aerosol climatology. In *Aerosol Forcingof Climate*; Charlson, R.J., Heintzenberg, J., Eds.; Wiley: New York, NY, USA, 1995.
55. Dusek, U.; Frank, G.P.; Hildebrandt, L.; Curtius, J.; Schneider, J.; Walter, S.; Chand, D.; Drewnick, F.; Hings, S.; Jung, D.; et al. Size matters more than chemistry for cloud-nucleating ability of aerosol particles. *Science* **2006**, *312*, 1375–1378. [CrossRef]
56. Reinmuth-Selzle, K.; Kampf, C.J.; Lucas, K.; Lang-Yona, N.; Fröhlich-Nowoisky, J.; Shiraiwa, M.; Lakey, P.S.J.; Lai, S.; Liu, F.; Kunert, A.T.; et al. Air pollution and climate change effects on allergies in the anthropocene: Abundance, interaction, and modification of allergens and adjuvants. *Environ. Sci. Technol.* **2017**, *51*, 4119–4141. [CrossRef]
57. Bruch, W.; Piazzola, J.; Branger, H.; Luneau, L.; Bourras, D.; Tedeschi, G.; van Eijk, A.M.J. Spray production dependence on wind and wave combinations: A tunnel study. *Bound. Layer Meteorol.* **2021**. in revision.
58. Piazzola, J.; Bouchara, F.; van Eijk, A.M.J.; de Leeuw, G. Development of the Mediterranean extinction code MEDEX. *Opt. Eng.* **2003**, *42*, 912–924. [CrossRef]
59. Wang, B.; Wu, H.; Wan, X.-F. Transport and fate of human expiratory droplets—A modeling approach. *Phys. Fluids* **2020**, *32*, 083307. [CrossRef] [PubMed]
60. Ma, Y.; Zhao, Y.; Liu, J.; He, X.; Wang, B.; Fu, S.; Yan, J.; Niu, J.; Zhou, J.; Luo, B. Effects of temperature variation and humidity on the death of Covid-19 in Wuhan, China. *Sci. Total Environ.* **2020**, *724*, 138226. [CrossRef] [PubMed]
61. Piazzola, J. *Rapport Intermédiaire T18 du Projet ANR-ASTRID "MATRAC", Juillet*; University of Toulon: Toulon, France, 2020.
62. Piazzola, J.; Mihalopoulos, N.; Canepa, E.; Tedeschi, G.; Prati, P.; Bastianini, M.; Zampas, P.; Missamou, T.; Cavaleri, L. Characterization of aerosols above the Northern Adriatic Sea: Case studies of offshore and onshore wind conditions. *Atmos. Environ.* **2016**, *132*, 153–162. [CrossRef]
63. Quan, F.-S.; Rubino, I.; Lee, S.-H.; Koch, B.; Choi, H.-J. Universal and reusable virus deactivation system for respiratory protection. *Sci. Rep.* **2017**, *7*, 39956. [CrossRef]
64. Fitzgerald, J.W. Approximation formulas for the equilibrium size for an aerosol particle as a function of its dry size and composition and the ambient relative humidity. *J. Appl. Meteorol.* **1975**, *14*, 1044–1049. [CrossRef]
65. Lewis, E.R.; Schwartz, S.E. *Sea Salt Aerosol Production: Mechanisms, Methods, Measurements and Models—A Critical Review*; American Geophysical Union: Washington, DC, USA, 2004; Volume 152, 413p.

66. Chan, K.H.; Malik Peiris, J.S.; Lam, S.Y.; Poon, L.L.M.; Yuen, K.Y.; Seto, W.H. The effects of temperature and relative humidity on the viability of the SARS coronavirus. *Adv. Virol.* **2011**, *7*. [CrossRef]
67. Kanji, Z.A.; Welti, A.; Corbin, J.C.; Mensah, A.A. Black carbon particles do not matter for immersion mode ice nucleation. *Geophys. Res. Lett.* **2020**, *46*, e2019GL086764. [CrossRef]